

Universal relations with fermionic dark matter

A. Krut^{1,2,3,*}, C. R. Argüelles^{3,5}, J. A. Rueda^{1,3,4}, and R. Ruffini^{1,3,4}

¹*Dip. di Fisica, Sapienza Università di Roma, Piazzale Aldo Moro 5, I-00185 Rome, Italy*

²*University of Nice-Sophia Antipolis, 28 Av. de Valrose, 06103 Nice Cedex 2, France*

³*ICRANet, Piazza della Repubblica 10, I-65122 Pescara, Italy*

⁴*ICRANet-Rio, Centro Brasileiro de Pesquisas Físicas, Rua Dr. Xavier Sigaud 150, 22290-180 Rio de Janeiro, Brazil*

⁵*Grupo de Astrofísica, Relatividad y Cosmología, Facultad de Ciencias Astronómicas y Geofísicas, UNLP and CONICET Paseo del Bosque S/N 1900, La Plata, Buenos Aires, Argentina*

Abstract. We have recently introduced a new model for the distribution of dark matter (DM) in galaxies, the Ruffini-Argüelles-Rueda (RAR) model, based on a self-gravitating system of massive fermions at finite temperatures. The RAR model, for fermion masses above keV, successfully describes the DM halos in galaxies, and predicts the existence of a denser quantum core towards the center of each configuration. We demonstrate here, for the first time, that the introduction of a cutoff in the fermion phase-space distribution, necessary to account for galaxies finite size and mass, defines a new solution with a compact quantum core which represents an alternative to the central black hole (BH) scenario for SgrA*. For a fermion mass in the range $48\text{keV} \leq mc^2 \leq 345\text{keV}$, the DM halo distribution fulfills the most recent data of the Milky Way rotation curves while harbors a dense quantum core of $4 \times 10^6 M_\odot$ within the S2 star pericenter. In particular, for a fermion mass of $mc^2 \sim 50\text{keV}$ the model is able to explain the DM halos from typical dwarf spheroidal to normal elliptical galaxies, while harboring dark and massive compact objects from $\sim 10^3 M_\odot$ to $10^8 M_\odot$ at their respective centers. The model is shown to be in good agreement with different observationally inferred universal relations, such as the ones connecting DM halos with supermassive dark central objects. Finally, the model provides a natural mechanism for the formation of supermassive BHs as heavy as few $\sim 10^8 M_\odot$. We argue that larger BH masses (few $\sim 10^{9-10} M_\odot$) may be achieved by assuming subsequent accretion processes onto the above heavy seeds, depending on accretion efficiency and environment.

1 Introduction

The problem of the distribution of stars in globular clusters, and more general in galactic systems, has implied one of the results of most profound interest in classical astronomy. In particular, in the pioneering works of [1] and [2], they considered the effects of collisional relaxation and tidal cutoff by studying solutions of the Fokker-Planck equation. There, it was shown that stationary solutions of this kind can be well described by lowered isothermal sphere models, based on simple Maxwellian energy distributions with a constant subtracting term interpreted as an energy cutoff. An extension of this statistical analysis with thermodynamic considerations, which includes the effects of violent (collisionless) relaxation, has been studied in [3], with important implications to the problem of virialization in galaxies which are still of actual interest. In a series of works, [4–6] changed the emphasis from self-gravitating systems of classic stars (which verify Maxwellian distributions) to systems of

fermionic particles with the aim of describing galactic dark matter halos. It was there considered a quantum fermionic distribution taking into account the possible presence of a cutoff in the energy as well as in the angular momentum. A remarkable contribution in the understanding of these issues was given in [7], based on the study of generalized kinetic theories accounting for collisionless relaxation processes, and leading to a class of generalized Fokker-Planck equation for fermions. It was there explicitly shown the possibility to obtain, out of general thermodynamic principles, a generalized Fermi-Dirac distribution function including an energy cutoff, extending the former results by [1] and [2] to quantum particles. More recently, it was shown that quantum particles fulfilling fermionic quantum statistics and gravitational interactions are able to successfully describe the distribution of galactic dark matter halos when contrasted with observations [8–11]. In particular, [11] proposed a new model (hereafter RAR model), based on such fundamental physical pillars to attack this problem, presenting a novel and more general *dense quantum core - classical*

*E-mail: e-mail: andreas.krut@icranet.org (ICRANet)

halo distribution. Thus, given the apparent ubiquity of massive black holes at the center of galaxies, in [11] the RAR model was proposed as a viable possibility to establish a link between the dark central cores to dark matter halos within a unified approach.

In this work we extend the RAR model by introducing a cutoff in the momentum distribution to account for finite galaxy sizes (analogously as previously done in [6]) and to account for more realistic galaxy relaxation mechanisms as indicated above and in [7]. This approach provides a new family of solutions with an overall redistribution of the bounded fermions. Consequently, the more stringent outer halo constraints of these novel configurations allow a higher compactness of the central cores. A detailed description of the presented results, the RAR model, its application to galactic structures and the comparison with universal relations is provided in [12].

2 Novel constraints from Milky Way Observables

We consider the extended high resolution rotation curve data of the Galaxy in [13], ranging from pc scales up to $\sim 10^2$ kpc, together with the orbital data of the eight best resolved S-cluster stars taken from [14]. Our analysis will thus cover in total more than nine orders of magnitude of radial extent.

As we will show below, the key result of our work is that there is a continuous underlying dark matter distribution covering the whole observed Galactic extent, which not only governs the dynamics of the outer halo above $r \gtrsim 10$ kpc, but also the central pc, being the intermediate region dominated by the baryonic components (bulge+disk).

The objective now is to solve the metric potential $\nu(r)$ for given regular initial conditions at the center (β_0, θ_0, W_0) and different dark matter particle mass m , in order to find the mass solution $M(r)$ consistent with the observationally constrained dark matter halo of the Galaxy. In detail, a dark matter halo described by $(r_1, M_1) = (40 \text{ kpc}, 2 \times 10^{11} M_\odot)$ consistent with the dynamics of the outer dark matter halo as shown recently in [15]. This is equivalently consistent with $(r_2, M_2) = (12 \text{ kpc}, 5 \times 10^{10} M_\odot)$ as constrained in [13]. Simultaneously, we require a quantum core of mass $M(r_c) = M_c = 4.2 \times 10^6 M_\odot$ enclosed within a radius $r_c \leq r_{p(S2)} = 6 \times 10^{-4} \text{ pc}$, the S2 star pericenter [14]. The results of this full boundary condition problem for the Milky Way observables are summarized in fig. 1.

The Milky Way outermost dark matter halo behavior is subjected to the cutoff conditions $W(r_b) \approx 0$ when $\rho(r_b) = 10^{-5} M_\odot/\text{pc}^3$ at the boundary radius $r_b = 50 \text{ kpc}$ (see fig. 1). Here, $\rho(r_b)$ is the Local Group density as constrained in [17]¹. The limiting behavior of such a dark matter density profile is also consistent with a dark matter halo mass of

¹Note that the exact $W(r) = 0$ cutoff condition, is fulfilled in the limiting case $\rho(r) = 0$ achieved for $r \gtrsim r_b$.

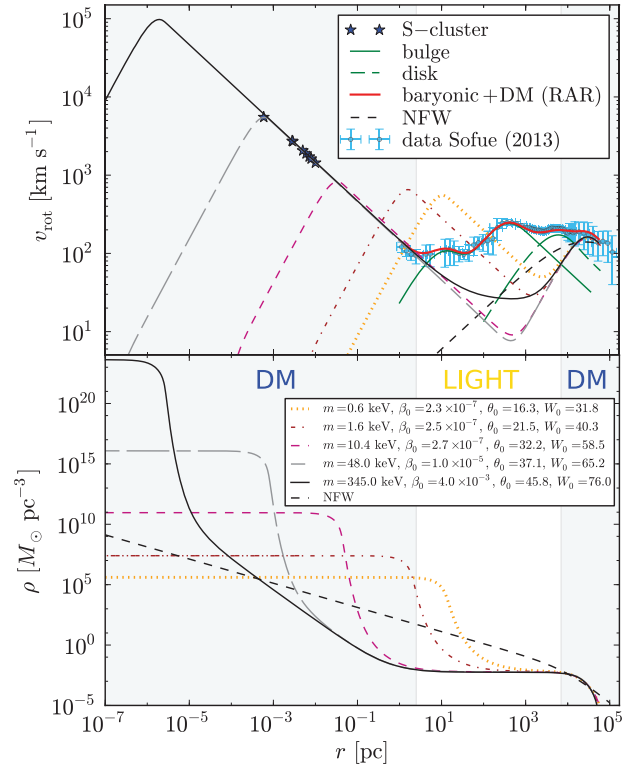


Figure 1. (Colour online, with permission of [12]) Theoretical rotation curves (upper panel) and density profiles (lower panel) for different DM fermion masses in the keV region, in agreement with all the Milky Way observables from $\sim 10^{-3}$ pc to $\sim 10^5$ pc. The continuous thick-red curve that fit the observed data (blue points) is the total rotation curve given by the RAR model plus the baryonic (bulge + disk) component without the need for a central BH, i.e. using any RAR profile for $mc^2 = 48\text{--}345$ keV. We also show, for the sake of comparison, the contribution of the NFW DM profile to the total rotation curve (not shown here) which produces an equally good fit to the data in the halo region [see 13, for details]. The stars-symbols represent the eight best resolved S-cluster stars [14], whose positions in the plot indicates the *effective* circular velocity at pericenter (i.e. without considering the ellipticity of the orbits). In the inner bulge region ($3 \lesssim r \lesssim 10^2$) pc, the large velocity error bars of about $\pm 20\text{--}30\%$ are mainly due to non-circular motions, while in the halo region there are larger observational errors bars of up to $\sim 50\%$ due to systematics [13]. The DM contribution to the Galactic halo becomes necessary above ~ 7 kpc, in agreement with [16].

$M(40 \text{ kpc}) = 2 \times 10^{11} M_\odot$ as required above, further implying a total Galactic mass (dark + baryonic) at r_b of $M_{\text{all}} \approx 3 \times 10^{11} M_\odot$, of which 80% is dark according to our model (i.e. $M(r_b) = 2.4 \times 10^{11} M_\odot$). It is clear that such a dark matter mass distribution must be also in agreement with the dynamical constraints set by the Galactic satellite dwarf observations, e.g. the Sagittarius (Sgr) dwarf satellite. Indeed, such observational constraints have been recently considered in [15], who showed that their fulfillment requires a total mass of the Galaxy (at $\sim 80\%$ confidence level)

$M_{\text{all}}(r \gtrsim 50 \text{ kpc}) \approx 3 \times 10^{11} M_{\odot}$, in agreement with our results here.

The different regimes in the $\rho(r)$ profiles are also manifest in the dark matter rotation curve. We define the first maxima as the core radius r_c and the second maxima as the halo (or the one-halo scale length) r_h . Following then the standard assumption in the literature that baryonic and dark matter do not interact each other, we have theoretically calculated the total rotation curve as $v_{\text{rot}}^2 = v_b^2(r) + v_d^2(r) + v_{\text{DM}}^2(r)$. With $v_b(r)$ and $v_d(r)$ the baryonic circular velocities for bulge and disk. We calculated the total (inner + main) bulge circular velocity using the same mass model parameters as in [13]. For the disk, we have performed the calculations with mass models parameters slightly changed (within 12%) with respect to those given in [13], where the NFW dark matter profile was assumed. We do this change to improve the fit of the observational data when adopting our dark matter profile. Finally, $v_{\text{DM}}^2(r)$ is the dark matter contribution given by the RAR model.

Varying the particle mass produces configurations which are classified in three groups. The fermion mass range $mc^2 \leq 10.4 \text{ keV}$ is firmly ruled out by the present analysis because the corresponding rotation curve exceeds the total velocity observed in the baryonic (bulge+disk) dominated region, between $\sim 1 \text{ pc}$ and 10^2 pc (including upper bound in error bars, see fig. 1).

In the intermediate range $10.4 \text{ keV} \lesssim mc^2 \lesssim 48 \text{ keV}$, the theoretical rotation curve is not in conflict with any of the observed data and dark matter inferences in [13], but the compactness of the quantum core is not enough to be an alternative to the central BH scenario.

There is a fermion mass range $48 \text{ keV} \lesssim mc^2 \lesssim 345 \text{ keV}$ with corresponding accompanying parameters (β_0, θ_0, W_0) , whose associated solutions explain the Galactic dark matter halo while providing at the same time an alternative for the central BH. The lower bound in m is imposed by the dynamics of the stellar S-cluster, while the upper bound corresponds to the last stable configuration before reaching the critical mass for gravitational collapse ($M_c^{\text{cr}} \sim m_{\text{Planck}}^3/m^2$, see also [18]). The critical configuration has a core radius $r_c \approx 4.75 r_{\bullet}$ with r_{\bullet} the Schwarzschild radius associated to a BH of $4.2 \times 10^6 M_{\odot}$ (see also [19]).

3 Comparing observed galaxy correlations

We turn now to analyze if the RAR model agrees with the $M_{\text{BH}} - M_{\text{tot}}$ relation [20–22] where M_{tot} is the total dark matter halo mass and M_{BH} is the mass of the compact dark object at the center of galaxies. Traditionally, that dark object is assumed as SMBHs but here interpreted as dark matter quantum cores in the case of inactive galaxies. In the following we consider $M_{\text{BH}} = M_c$, being $M_c = M(r_c)$ the quantum core mass. In order to show this, we use the full family

of RAR solutions for typical dSphs ($r_h = 0.26 \text{ kpc}$, $M_h = 2.7 \times 10^7 M_{\odot}$), spiral ($r_h = 48 \text{ kpc}$, $M_h = 1 \times 10^{12} M_{\odot}$) and elliptical galaxies ($r_h = 90 \text{ kpc}$, $M_h = 5 \times 10^{12} M_{\odot}$) calculated for the particle mass $mc^2 = 48 \text{ keV}$ and spanning the maximal free parameter space (β_0, θ_0, W_0) in each galaxy case. See [12] for details. These solutions cover correspondingly a well defined window of predicted masses (M_c, M_{tot}) summarized in fig. 2.

For typical spiral and elliptical galaxy types the family of predicted (M_c, M_{tot}) covers the (horizontal) spread of the observed correlation for each galaxy type. In addition, it extends out of it indicating a window of predicted masses by the RAR model, not yet observed. The limiting values of (M_c, M_{tot}) , with observationally given halo radius r_h and halo mass M_h , are automatically established by the gravitational core collapse at the critical point (intrinsic physical condition) and the necessity to have a dark matter density contribution above the galaxy group-scale (astrophysical condition). The Milky Way RAR-solution is also plotted for completeness showing a good agreement as well. The (M_c, M_{tot}) RAR-predictions are displayed together with the observationally inferred best-fit relations [20, 22], only in the region where data supports (i.e. the so-called Ferrarese window in fig. 2). The case of typical dwarf galaxies is located at the lower end of the (M_c, M_{tot}) plane. It is worth to stress that no observational data exist yet in that part of the correlation and thus the blue curve at the bottom of fig. 2 is a prediction of the RAR model. Additional verification of the above predictions of the RAR model needs the observational filling of the gaps in the (M_c, M_{tot}) plane from dwarfs all the way up to ellipticals. This is a work in progress within our group.

It is appropriate at this point to recall that the majority of the values of M_{BH} in the observed $M_{\text{BH}} - M_{\text{tot}}$ relation have been obtained through the so-called $M_{\text{BH}} - \sigma_*$ relation, with σ_* the bulge dispersion velocity [23–25]. The M_{tot} values were there calculated at the virial radius within a Navarro-Frenk-White dark matter model [20] while in our case they were obtained at the boundary radius r_b of the RAR model equilibrium configurations. In the case of dwarf galaxies the observational inference of the mass of the central dark region via the dispersion velocity is unclear [see, e.g., 21, 26, and references therein]. However, [26] attempted to give an estimate of the dark central object mass in dwarf galaxies obtaining $M_{\text{BH}} \sim 10^3 - 10^4 M_{\odot}$ (often called intermediate massive BHs), in agreement with the values of M_c for dSph analyzed in this work. Special attention has to be given to our dwarf galaxy predictions in view of the recent observational result reported in [27] on the putative massive black holes of few $\sim 10^6 M_{\odot}$ detected in ultra-compact dwarf galaxies of total mass of few $\sim 10^7 M_{\odot}$. Interestingly, these (rather evolved) compact dwarf galaxies show no (observational) hints of being dominated by a dark matter halo, remarkably in agreement with

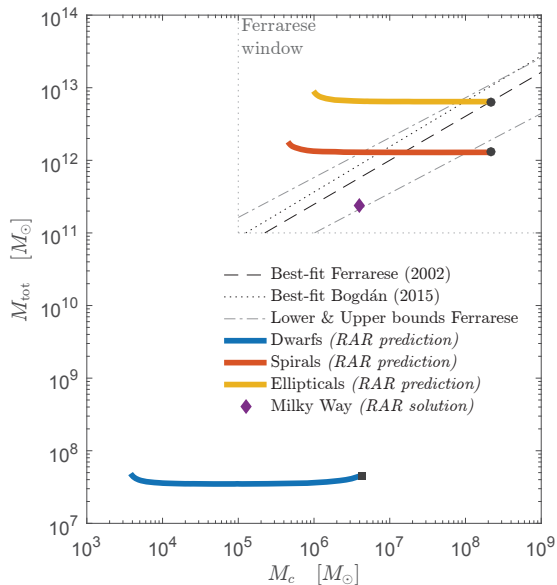


Figure 2. (Colour online, with permission of [12]) The different *predicted* colour lines read for each galaxy type showing the ability of the three parametric (β_0, θ_0, W_0) RAR solutions for a particle mass $mc^2 = 48$ keV to be in agreement with the different $M_{\text{BH}} - M_{\text{tot}}$ relations considered in the literature (see text) and explicit in the picture box. While the red and yellow RAR prediction lines, together to the Milky Way solution (i.e. spiral and elliptical galaxies) lay within the *observable Ferrarese window*, the blue RAR prediction for dwarfs, is located at the lower end of the $M_c - M_{\text{tot}}$ plane, where data do not support. The black dots correspond to the critical core masses M_c^{cr} , the black square indicates the limiting maximum core mass for dwarfs M_c^{max} .

our *halo deficit*² solution, see fig. 2. It is interesting that this observational inference was published few weeks after the completion of our predictions. This is a potentially important prediction of the RAR model which deserves further analysis.

Moving to the larger elliptical galaxies, it is interesting to note that the maximum quantum core mass $M_c^{cr} \sim 2 \times 10^8 M_\odot$ (for $mc^2 = 48$ keV) predicted by our model, is in striking consistency with the uppermost (sample-representative) central mass M_{BH} obtained from an X-ray imaging analysis of more than 3000 isolated and inactive elliptical galaxies [22]. These results, when viewed through our theoretical $M_c - M_{\text{tot}}$ relation, give support to our idea that normal elliptical galaxies may harbor dark central objects (not yet BHs) without showing AGN-like activity, while larger SMBHs masses do show AGN properties and thus reach the upper end of the $M_{\text{BH}} - M_{\text{tot}}$ relation.

²This has to be understood in a technical context rather than in an astrophysical.

4 Conclusion

It is now clear from our results that gravitationally bounded systems based on fermionic phase-space distributions including for escape velocity effects and central degeneracy, can explain the DM content in the Galaxy while providing a natural alternative for the central BH scenario in SgrA*. A key point of the present RAR model is the ability to predict entire DM halo configurations which fulfil the observed properties of galaxies, such as the $M_{\text{BH}} - M_{\text{tot}}$, for a unique DM fermionic mass. At the same time it provides, on astrophysical basis, possible clues on the formation of super massive BHs in galactic nuclei.

Our general results on the DM distribution in galaxies can be considered as complementary to those based on standard cosmological simulations. However, the latter being based on N-body purely Newtonian simulations, contrast with our semi-analytical four-parametric approach which has the chance to include more rich physical ingredients, such as quantum statistics (arising from specific phase-space relaxation mechanisms), thermodynamics and gravity. We have shown that our density profiles successfully agree with a large variety of galactic observables and universal laws.

An important aspect of the particle mass range of few 10–100 keV obtained here from galactic observables is that it produces basically the same behavior in the power spectrum (down to Mpc scales) from that of standard Λ CDM cosmologies, thus providing the expected large-scale structure (see for details [28]). In addition, it is not *too warm* (i.e. our masses are larger than $mc^2 \sim 1-3$ keV) to enter in tension with current Ly α forest constraints [29, 30] and the number of Milky Way satellites [31] as in standard Λ WDM cosmologies.

All the above arguments offer significant support for our keV-scale fermions as dark matter, which may well co-exist harmonically with other DM species in the universe. These aspects will have to interplay with the physics of elementary particles regarding the nature of these fermions (Majorana neutrinos, supersymmetric particles, sterile neutrinos, etc.) as well as with the possible detection through decaying processes involving weak interactions. Indeed, DM fermion masses within the relatively narrow window obtained here, $48 \text{ keV} \lesssim mc^2 \lesssim 345 \text{ keV}$, have also arisen within different microscopic models based on extensions of the standard model and consistent with all cosmological (i.e. large scale structure) and X-ray constraints as the ones considered in [29].

Acknowledgments

A. K. is supported by the Erasmus Mundus Joint Doctorate Program by Grants Number 2014-0707 from the agency EACEA of the European Commission.

References

- [1] R.W. Michie, *MNRAS***125**, 127 (1963)
- [2] I.R. King, *AJ***71**, 64 (1966)
- [3] D. Lynden-Bell, *MNRAS***136**, 101 (1967)
- [4] R. Ruffini, L. Stella, *A&A***119**, 35 (1983)
- [5] J.G. Gao, M. Merafina, R. Ruffini, *A&A***235**, 1 (1990)
- [6] G. Ingrosso, M. Merafina, R. Ruffini, F. Strafella, *A&A***258**, 223 (1992)
- [7] P.H. Chavanis, *Physica A Statistical Mechanics and its Applications* **332**, 89 (2004), [cond-mat/0304073](#)
- [8] H.J. de Vega, P. Salucci, N.G. Sanchez, *MNRAS***442**, 2717 (2014), [1309.2290](#)
- [9] C.R. Argüelles, R. Ruffini, I. Siutsou, B. Fraga, *Journal of Korean Physical Society* **65**, 801 (2014), [1402.0700](#)
- [10] I. Siutsou, C.R. Argüelles, R. Ruffini, *Astronomy Reports* **59**, 656 (2015), [1402.0695](#)
- [11] R. Ruffini, C.R. Argüelles, J.A. Rueda, *MNRAS***451**, 622 (2015), [1409.7365](#)
- [12] C.R. Argüelles, A. Krut, J.A. Rueda, R. Ruffini, *ArXiv e-prints* (2017), [1606.07040](#)
- [13] Y. Sofue, *PASJ***65**, 118 (2013), [1307.8241](#)
- [14] S. Gillessen, F. Eisenhauer, T.K. Fritz, H. Bartko, K. Dodds-Eden, O. Pfuhl, T. Ott, R. Genzel, *ApJ***707**, L114 (2009), [0910.3069](#)
- [15] S.L.J. Gibbons, V. Belokurov, N.W. Evans, *MNRAS***445**, 3788 (2014), [1406.2243](#)
- [16] F. Iocco, M. Pato, G. Bertone, *Nature Physics* **11**, 245 (2015), [1502.03821](#)
- [17] Y. Sofue, *PASJ***64**, 75 (2012), [1110.4431](#)
- [18] C.R. Argüelles, R. Ruffini, *International Journal of Modern Physics D* **23**, 1442020 (2014), [1405.7505](#)
- [19] C.R. Argüelles, R. Ruffini, B.M.O. Fraga, *Journal of Korean Physical Society* **65**, 809 (2014), [1402.1329](#)
- [20] L. Ferrarese, *ApJ***578**, 90 (2002), [astro-ph/0203469](#)
- [21] J. Kormendy, R. Bender, *Nature***469**, 377 (2011), [1101.4650](#)
- [22] Á. Bogdán, A.D. Goulding, *ApJ***800**, 124 (2015), [1502.05043](#)
- [23] L. Ferrarese, D. Merritt, *ApJ***539**, L9 (2000), [astro-ph/0006053](#)
- [24] K. Gebhardt, R. Bender, G. Bower, A. Dressler, S.M. Faber, A.V. Filippenko, R. Green, C. Grillmair, L.C. Ho, J. Kormendy et al., *ApJ***539**, L13 (2000), [astro-ph/0006289](#)
- [25] K. Gültekin, D.O. Richstone, K. Gebhardt, T.R. Lauer, S. Tremaine, M.C. Aller, R. Bender, A. Dressler, S.M. Faber, A.V. Filippenko et al., *ApJ***698**, 198 (2009), [0903.4897](#)
- [26] M. Valluri, L. Ferrarese, D. Merritt, C.L. Joseph, *ApJ***628**, 137 (2005), [astro-ph/0502493](#)
- [27] C.P. Ahn, A.C. Seth, M. den Brok, J. Strader, H. Baumgardt, R. van den Bosch, I. Chilingarian, M. Frank, M. Hilker, R. McDermid et al., *ApJ***839**, 72 (2017), [1703.09221](#)
- [28] A. Boyarsky, O. Ruchayskiy, M. Shaposhnikov, *Annual Review of Nuclear and Particle Science* **59**, 191 (2009), [0901.0011](#)
- [29] A. Boyarsky, J. Lesgourgues, O. Ruchayskiy, M. Viel, *Physical Review Letters* **102**, 201304 (2009), [0812.3256](#)
- [30] M. Viel, G.D. Becker, J.S. Bolton, M.G. Haehnelt, *Phys. Rev. D***88**, 043502 (2013), [1306.2314](#)
- [31] E.J. Tollerud, J.S. Bullock, L.E. Strigari, B. Willman, *ApJ***688**, 277-289 (2008), [0806.4381](#)